

ADA063751

LEVEL

(13)

Technical Note

1978-79

Minimum False-Source Detection
Capacities of Two-Dimensional,
Scanned, Optical Detector Arrays
in Constant False-Alarm Systems

L. W. J. J.

30
JAN 1980

3 November 1979

Prepared for the Department of the Air Force
Contract AF-33(616)-79-1-0002

Lincoln Laboratory

MASSACHUSETTS INSTITUTE OF TECHNOLOGY
LINCINN, MASSACHUSETTS

30
JAN 1980

Approved for public release; distribution unlimited

The work reported in this document was performed at Lincoln Laboratory, a center for research operated by Massachusetts Institute of Technology, with the support of the U.S. Air Force under Contract F19628-79-4-0001.

This report may be reproduced to satisfy needs of U.S. Government agencies.

The views and conclusions contained in this document are those of the author(s) and should not be interpreted as necessarily representing the official policies, either expressed or implied, of the United States Government.

This technical report has been reviewed and is approved for publication.

FOR THE COMMANDER

John J. O'Donoghue, Jr.

Major General, USAF

Lincoln Laboratory, Bedford, Mass.

LEVEL

12

MASSACHUSETTS INSTITUTE OF TECHNOLOGY
LINCOLN LABORATORY

LIMITING POINT-SOURCE DETECTION
CAPABILITIES OF TWO-DIMENSIONAL,
SCANNED, OPTICAL DETECTOR ARRAYS
IN CONSTANT FALSE-ALARM SYSTEMS

R. WEBER

Group 94

TECHNICAL NOTE 1978-10

3 NOVEMBER 1978

ADDITIONAL TO	
DTIC	State Center <input checked="" type="checkbox"/>
DDC	DDC Center <input type="checkbox"/>
UNCLASSIFIED	<input type="checkbox"/>
JUSTIFICATION	
BY	
DISTRIBUTION/AVAILABILITY CODES	
Dist.	AVAIL. and/or SPECIAL
A	


Approved for public release; distribution unlimited.

DDC
RECEIVED
JAN 26 1979
D

LEXINGTON


MASSACHUSETTS

79 01 22 049



ABSTRACT

An optical point-source detection system in which a constant number of false alarms is allowed per data set (exposure time) based on the post-detection processing, is considered. The detector is a two-dimensional scanned array. With a single threshold determined solely by the allowed false alarms, that minimum average signal necessary to satisfy a given requirement on the probability of detection for various background (sky, in this instance) and electronic noise levels is determined. This development leads to a critical signal-noise expression at the first photon to charge-carrier conversion surface which is not an explicit function of the standard deviation of the signal. This expression is used to compare the detection performances of noise-free and of noisy detector arrays using the parameters of typical, ground-based, satellite surveillance systems.



LIMITING POINT-SOURCE DETECTION CAPABILITIES OF TWO-DIMENSIONAL, SCANNED, OPTICAL DETECTOR ARRAYS IN CONSTANT FALSE-ALARM SYSTEMS

The intention of the present Note is to develop by straight-forward means an operational expression for the signal-to-noise ratio at the first photon-to-charge-carrier conversion surface of a two-dimensional scanned detector array in a system in which a single threshold, based solely on an allowed number of false alarms per exposure, is to be set, and in which the average value of the signal must be such as to provide a required probability of detection. Such an expression will facilitate the prediction of array performance and the comparison of array performance in systems of this type.

It is convenient to bear in mind the general type of system that is under consideration. Optical flux from a distant point-source (e.g., star or satellite) and from the sky background are collected by means of a telescope. At the first conversion surface - either a photoemissive surface or the solid-state array itself - which lies in the focal plane of the telescope, the focused photons are converted to charge carriers which are eventually "read out" by a two-dimensional scanning mechanism. At the point of read-out, instrument noise is introduced. All calculations are to be performed on an image-cell basis at the first conversion surface.

It is customary to define the size of an image cell from the full linewidth at half-amplitude of the read-out (video) point-source signal. This time may then be converted to a field-of-view per image cell,

usually expressed in square arc-seconds¹. All signal counts and noise counts per image cell may then be referred to the first conversion surface of the detector. This is a convenient procedure for the purpose at hand: The signal-to-noise ratio calculated at this surface represents the maximum achievable value for the given system under a given set of operating conditions and is thus the ideal point at which to gauge performances or to make comparisons of different detectors.

Figure 1 defines the relevant parameters involved at an image cell at the first conversion surface. All quantities are in counts per exposure time per cell, unless noted otherwise. A square image cell has been assumed. These quantities will be given greater definition as the discussion proceeds.

In an image cell not containing signal counts, sky noise and instrument noise combine to yield a distribution whose standard deviation is given by $\sigma_n = \sqrt{\sigma_B^2 + N^2}$. The average value of this distribution is to be used as a reference level which, as a practical matter, may be assumed to be zero. The signal quantity \bar{S} includes in its total fluctuation, σ , both σ_n and the classical signal fluctuation σ_s and is given by $\sigma = \sqrt{\sigma_n^2 + \sigma_s^2}$. An illustration of the situation is presented in Figure 2.

The dashed vertical line, located at d in Figure 2, represents a threshold that has been determined by an acceptable false alarm level for a given signal processing scheme. In addition to the acceptable false-alarm probability, P_{FA} , a probability of detection, P_D , requirement shall be assumed imposed on the system. One then asks: Given the

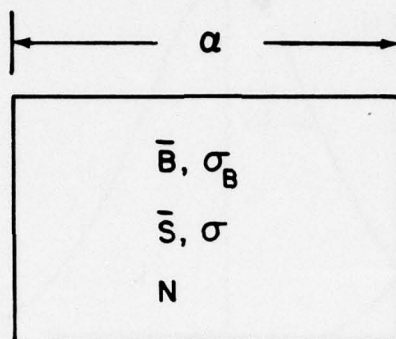


IMAGE CELL:

 α : WIDTH IN SEC

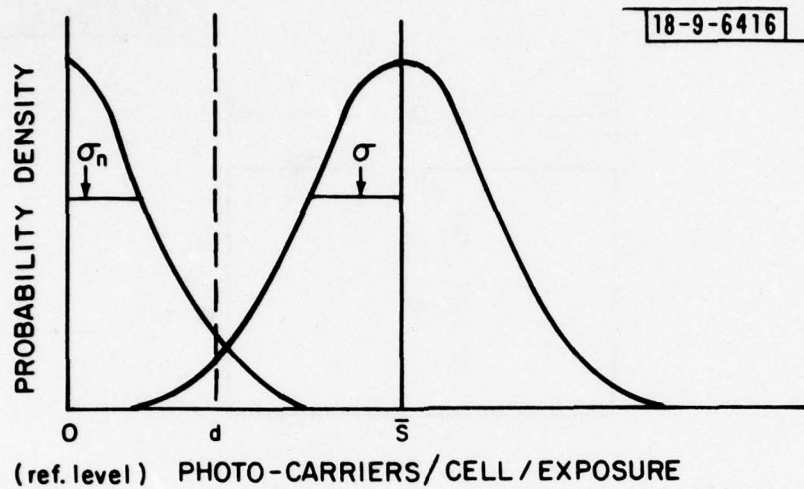
SIGNAL QUANTITIES:

 \bar{S} : AVERAGE SIGNAL COUNT σ : TOTAL FLUCTUATION OF SIGNAL

NON-SIGNAL QUANTITIES:

 \bar{B} : AVERAGE SKY-BACKGROUND COUNT σ_B : FLUCTUATION OF B N : RMS INSTRUMENT NOISE ELECTRON COUNT

Fig. 1. Relevant parameters in a first-surface image-cell per exposure time.



$$\sigma_n = \sqrt{\sigma_B^2 + N}$$

$$\sigma = \sqrt{\sigma_n^2 + \sigma_s^2}$$

Fig. 2. Noise-background and signal distributions. (See Figure 1 for definitions of symbols.)

acceptable P_{FA} and the required P_D for a given system, what minimum values of the average signal, \bar{S}_m , are required for various values of the background? In terms of a satellite detection system, the question may be rephrased as follows: What minimum satellite brightnesses (maximum visual magnitudes) are detectable with a specific detector for a given set of system requirements (P_{FA} and P_D) and operational parameters (e.g., fields of view, exposure times, and night-sky brightnesses)?

Let us assume that for an acceptable number of false alarms per exposure, d must be set at $k \sigma_n$ above the mean reference level. For the desired probability of detection P_D , then, \bar{S} must exceed d by $j \sigma$. This leads to the necessary minimum value of \bar{S} for the required P_{FA} and P_D , and for the given σ_n :

$$\bar{S}_m = k \sigma_n + j \sigma. \quad (1)$$

For $\bar{S} > \bar{S}_m$ and fixed σ_n^\dagger , and k , the false-alarm-fill over the array remains constant but P_D increases.

Expanding Equation (1) yields:

$$\bar{S}_m = k \sigma_n + j \sqrt{\sigma_n^2 + \sigma_s^2}. \quad (2)$$

With the assumption that fluctuations in the optical radiation field may be neglected, the substitution of $\sigma_s^2 = \bar{S}$ may be made in Eq. (2). Upon rearrangement and squaring, there results a quadratic equation

$$\overline{\sigma_n} = \sigma_n(t)$$

in \bar{S}_m . The solution yields $\bar{S}_m = \bar{S}_m(\sigma_n; j, k)^\dagger$. An important point is clear. \bar{S}_m , once k and j have been chosen, does not depend explicitly on the signal fluctuation σ_s . To demonstrate this, and since it is a condition that has been used in the field, let us now assume that $k = j$. Then,

$$\bar{S}_m = 2k \sigma_n + k^2. \quad (3)$$

Equation (3) indicates that \bar{S}_m depends on the processing scheme (i.e., on the selected value of k), as mentioned, and on the combined fluctuations of the sky background and instrument noise (through σ_n). Equation (3), as well as the more general expression for $k \neq j$,[†] also indicates that the sought after first-conversion-surface signal-to-noise ratio is given by \bar{S}_m/σ_n .

Since the condition that $k = j$ has been used to derive Equation (3), the probability of detection, P_D , is simply related to the probability of false alarm, P_{FA} , through the relation $P_D = 1 - P_{FA}$. For the ETS-tested TRW AMTI system², d was set at approximately $1.65 \sigma_n$. For $k = j = 1.65$, 95 percent of the noise peaks fall below d and a similar percentage of the signal fluctuations exceed d . The latter percentages refer to Gauss statistics; for Poisson statistics, the situation is improved somewhat because of the asymmetry of the distribution.

For $k = j = 1.65$,

$$\bar{S}_m = 3.30 \sigma_n + 2.72. \quad (4)$$

[†] See Appendix

As a reference point, it seems reasonable to assume the minimum value of σ_n per exposure to be unity. Then, using Equation (4), $\bar{S}_m/\sigma_n = 6.02$ for the specified performance. For $\bar{S} < \bar{S}_m$, performance is degraded: P_D decreases. For $\bar{S} > \bar{S}_m$ and fixed σ_n , P_D increases. If constant performance (CP) is desired as σ_n increases, that is, the number of false alarms per data set and the probability of detection are to remain constant, the required value of \bar{S}/σ_n decreases. In fact, for very large σ_n (and \bar{S}), \bar{S}/σ_n approaches 3.30 for the present choice of k . This fall-off in the required value of \bar{S}_m/σ_n as σ_n (and \bar{S}) increases is a consequence of the fact that the ratio σ_s/\bar{S} decreases as \bar{S} increases.

Figure 3 shows constant performance (CP) plots of Equation (3) for $k = j = 1.65$ and for $k = j = 2.50$. The former values are for $P_{FA} \approx 5.0$ percent and $P_D \approx 95$ percent while the latter are for $P_{FA} \approx 0.5$ percent and $P_D \approx 99.5$ percent. For $k = j = 2.50$, $\bar{S}_m/\sigma_n = 11.25$ for $\sigma_n = 1$. Clearly, an increase in σ_n (for small σ_n) requires a lesser increase in \bar{S} if the level of performance is to be maintained.

The straight-line plots on Figure 3 are for the case of constant first-surface signal-to-noise ratio (CSNR). This situation is realized when the signal-to-noise ratio remains constant at its S_m/σ_n ($\sigma_n = 1$) value as the background level (and signal level) increases. P_{FA} is to remain constant while P_D increases. Here, for fixed k and σ_n , the required value of \bar{S} is greater than in the corresponding CP case. In

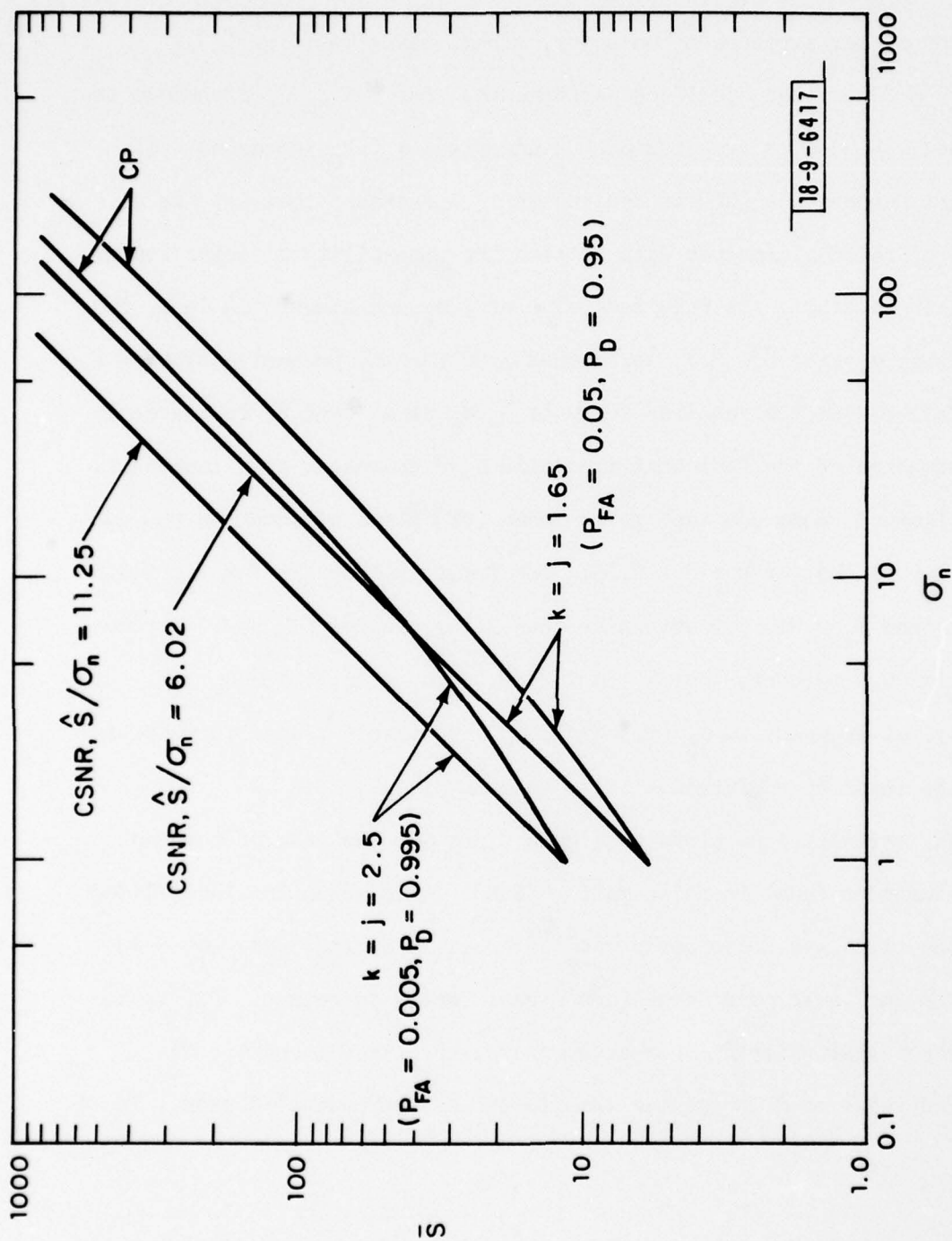


Fig. 3. Average signal vs noise standard deviation for constant performance (CP) and for constant first-surface signal-to-noise (CSNR) cases.

the comparison of a detector array in which $N = 0$ with one in which $N \neq 0$, the latter suffers more in the CSNR situation than in the CP situation.

At this point, to repeat, the original intention of the present Note has been satisfied: for detection schemes in which a decision threshold is set to realize an acceptable level of false alarms and in which the average signal counts must be such as to provide the required probability of detection, the first-surface signal-to-noise ratio \bar{S}/σ_n , where σ_n depends only on the sky-background and the electronic noise in an image cell, is a useful quantity with which to gauge performance. The major assumptions are that there is a reference level from which a false alarm threshold may be set and that variances equal average values (e.g., $\sigma_s^2 = \bar{S}$). Both assumptions are reasonable. Conceptually, the time-sequential readout of the array may be used to facilitate the determination of the dc noise (sky plus instrument) reference level. This is possible since, in general, the vast majority of the cells of a two-dimensional array contain noise while the remainder may contain signal-plus-noise. The assumption that Poisson statistics adequately describe the photo-conversion process is reasonable since the number of anticipated counts is small. This is especially true should the limits of detection be sought for sufficiently short integration times (sufficiently high sampling rates).

It is to be emphasized that while the first-surface signal-to-noise ratio, \bar{S}/σ_n , contains the quantity \bar{S} , it is highly unlikely that in a single short exposure the average value of S would ever be realized (or more importantly, recognized as such). However, the setting of the false alarm threshold necessarily results in the desired probability of detection over a number of data sets for an appropriate average number of signal counts. It is evident, then, that simple detection of the type discussed - involving relatively short exposure times - is not compatible with photometry which requires the determination of the average number of signal counts with reasonable accuracy. The only recourse is to spend more time, perhaps by the integration of many short exposures each taken at the appropriate time during the unfolding of the signature of the object. Once means are at hand to provide a measure of the signal average, the statement that the uncertainty of the measurement (\pm) is of the order of the reciprocal of the signal-to-noise ratio applies.

The reader who is not interested in the comparison of the point-source detection capability of a bare array with that of an intensified array should, at this point, pass to the Appendix for analytical expressions for P_{FA} , P_D and \bar{S} , with $k \neq j$.

The plan now is to compare the performance of a bare CCD array (B-CCD) with that of an intensified CCD array (I-CCD). The pre-array current intensification shall be assumed sufficient to reduce the instrument electronic rms noise (N) in an image cell at the first conversion surface to a small, negligible value. For the present purpose, the variable is to be the value of N associated with the B-CCD.

The conditions for the comparison are as follows:

- Effective area of telescope:

$$0.29 \text{ m}^2 (\approx \text{ETS } 31", f/5)$$

- Broadband solar quantum efficiency of B-CCD:

40 percent (silicon)

- Broadband solar quantum efficiency of I-CCD:

7.2 percent (S-20)

- Signal reference point:

15^{m} G-star, zero air mass, provides 5.00×10^4
photons/meter²/sec at the aperture of the telescope³.

The point signal is assumed to fall in a single
image cell (for convenience).

- The night-sky-brightness, NSB, (assumed sun-like)

is to be 19.5 sec^{-2} .

- The number of image cells is to be such that the

angular area of each is to be 2.56 sec^2 .

(≈ 32 .cells/mm in the focal plane).

The following values, obtained from the above conditions, indicate
the one-second charge-carrier "counts" per referred image cell:

	Signal, \bar{S}	NSB
B-CCD	5900.	240.
I-CCD	1030.	42.

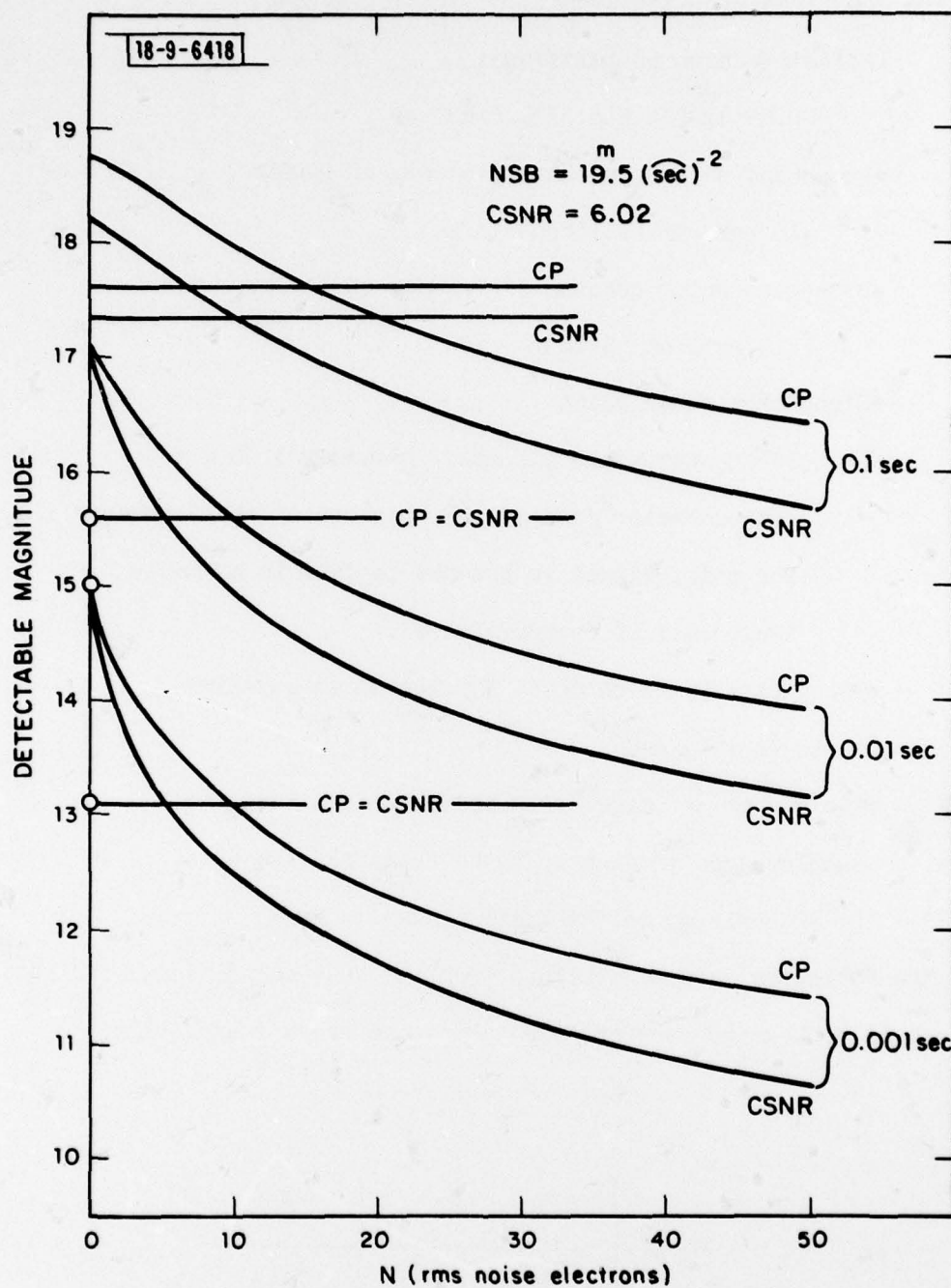


Fig. 4. Detectable magnitude vs rms noise electrons for several short exposure times and for two cases. (See text for description.)

In the calculations (using Equation (4)) the integration (exposure) times considered were 0.1 s, 0.01 s, and 0.001 s. Both CP and CSNR were considered with the minimum detectable average signal, \bar{S}_m , determined with $k = j = 1.65$, providing a P_{FA} of 5 percent and a P_D of 95 percent per exposure (GEODSS' specified values). Figure 4 indicates the results in terms of detectable point-source magnitude versus instrument rms noise electrons per image cell, N , at the first conversion surface. The horizontal lines represent the performance of the I-CCD ($N = 0$) for the various exposure times. The pairs of curves show the expected performance of the B-CCD for the various exposure times as a function of N . The upper curve in each pair represents constant performance (CP); the lower, constant first-surface signal-to-noise ratio (CSNR). The three encircled points on the ordinate are points for which the detection capability has been limited by the condition that $(\sigma_n)_{\min.} = 1$.

Equal-performance cross-over points are given by the intersections of the horizontal lines with the curves. For example, for the CP case and an exposure time of 0.1 sec, the cross-over occurs for $N \approx 15$ while for the same time and for the CSNR case it occurs for $N \approx 10$. For values of N greater than 15, then, the I-CCD outperforms the B-CCD for an exposure time of 0.1 s in either case. For $N = 15$, the current gain required of the I-CCD to insure that the referred noise be much less than unity is approximately 150, an easily realizable value.

For exposure times of 0.01 s and 0.001 s, the I-CCD outperforms the B-CCD, for both CP and CSNR cases, for $N > 10$ and for $N > 5$, respectively. Then, the maximum required current gain is approximately 100.

The following table compares the performance of an I-CCD with that of a B-CCD with $N = 30$, a realistic value. The required current gain in each case is approximately 300.

	Exposure Time (sec.)	Limiting Detectable Magnitude	Δ Magnitude
CP I/B CSNR I/B	0.1 ↓	17.65/16.95 17.35/16.30	0.70 1.05
CP I/B CSNR I/B	0.01 ↓	15.60/14.40 15.60/13.70	1.20 1.90
CP I/B CSNR I/B	0.001 ↓	13.10/11.90 13.10/11.20	1.20 1.90

CP = constant performance ($P_{FA} = 0.05$, $P_D = 0.95$)

CSNR = constant first surface signal-to-noise ratio (6.02 in this example)

I = intensified CCD with $G_{max} \approx 300$.

B = bare CCD

$N = 30$ rms electrons

$NSB = 19.5 \text{ sec}^{-2}$

A more general feeling for the relative performances of the arrays may be realized by the use of Equation (4), in the constant-performance (CP) case. Equating the I-CCD and the B-CCD versions of Equation (4) should yield the loci of equal performance:

$$\frac{3.30[\varphi_B A_T t \alpha^2 \eta_I]^{1/2} + 2.72}{\eta_I} = \frac{3.30[\varphi_B A_T t \alpha^2 \eta_B + N^2]^{1/2} + 2.72}{\eta_B} \quad (5)$$

In this expression, φ_B is the night-sky flux rate, A_T is the effective (0-obscuration, 100 percent T) area of the telescope, t is the integration time, α^2 is the angular area of the image cell, η_I is the broadband, solar quantum efficiency of the photo-conversion surface of the I-CCD, η_B is the similar quantity for the B-CCD, and N^2 represents the mean-square electron noise count per cell in the B-CCD. The noise count for the I-CCD has been taken to be negligible.

With the substitutions $K \equiv \varphi_B A_T t \alpha^2$, $c = \eta_B/\eta_I$, and $L = (K\eta_I)^{1/2} + 0.82$, Equation (5) may be solved for c :

$$c = \frac{1}{2L^2} [(1.64L + K\eta_I) + (1.64L + K\eta_I)^2 + 4L^2(N^2 - 0.67)] \quad (6)$$

Now, $K\eta_I$ is the photoelectron σ_n^2 for the I-CCD case. For assumed values of $\sigma_n^2 = K\eta_I = \varphi_B A_T t \alpha^2 \eta_I$, Equation (6) may be solved for c for selected values of N . The results are given as Figure 5 with η_I assumed to be 0.07, representative of an S-20 surface. Given σ_n^2 , each curve indicates the maximum allowed N for a given η_B for equal performances of

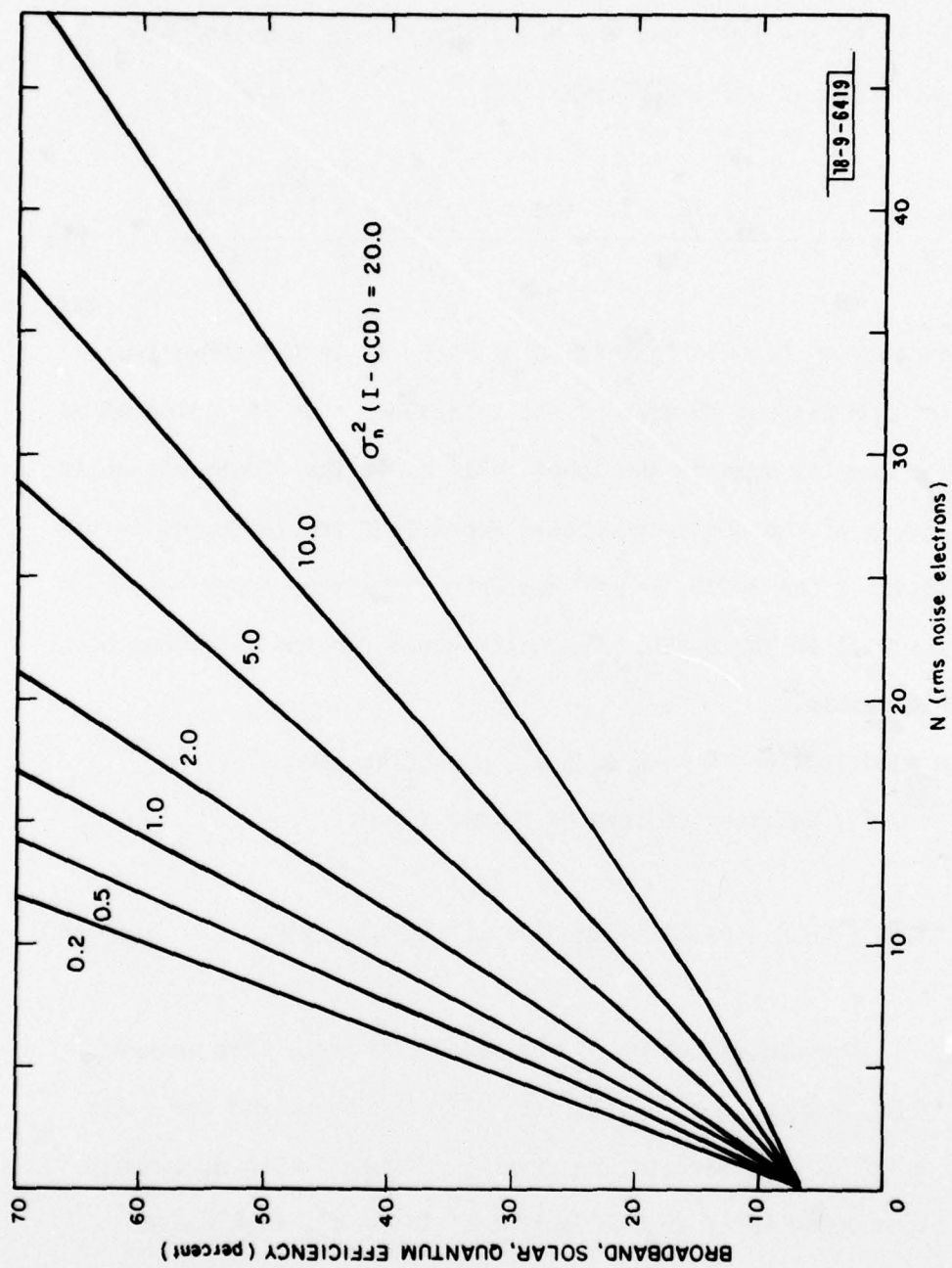


Fig. 5. Broadband solar quantum efficiency vs noise electrons of a bare array for equal performance of an intensified array, with noise variance of the latter as a parameter. (See text for description.)

the I- and B-CCD arrays. For example, for $\sigma_n^2 = 10.0$ and $\eta_B = 40$ percent, the I-CCD is superior to the B-CCD for $N \gtrsim 21$ rms electrons per cell. For convenience, the following table indicates typical values of σ_n^2 (S-20) for a $19^m.3$ sky, for an image-cell size of 2.56 sec^2 , for several exposure times, and for the ETS 31" telescope.

t (sec)	σ_n^2 (S-20)
0.1	5.
0.01	0.5
0.001	0.05

For $t = 0.01 \text{ s}$ and $\eta_B = 40$ percent, Figure 5 indicates that the I-CCD is preferred for $N \gtrsim 8$ rms electrons per cell. With the above table, and since $\sigma_n^2 = \phi_B A_T t \alpha^2 \eta_I$, many combinations may be considered. First, suppose all is as in the preceding example except that α^2 is increased to 10.24 sec^2 (a factor of 4). Then, $\sigma_n^2 = 2.0$. Figure 5 indicates that the I-CCD is superior for $N \gtrsim 12$. If now one considers the GEODSS main telescope with approximately twice the effective area of the ETS telescope, $\sigma_n^2 = 4.0$ and the I-CCD outperforms the B-CCD imager for $N \gtrsim 15$. Finally, extending the last example, but specifying $N = 30$, σ_n^2 may become as large as 24, approximately, before the B-CCD outperforms the I-CCD. Then, the sky brightness would be almost as bright as $17^m.3 \text{ sec}^{-2}$.

It should be noted once more that if the case of constant, first-surface, signal-to-noise ratio (CSNR) were to be considered, the bare CCD would not do as well as indicated in the above considerations.

In conclusion, it has been shown that if a detection threshold, based on an acceptable false alarm level is set and if \bar{S} is such as to provide a desirable probability of detection per exposure, the quantity \bar{S}/σ_n , where \bar{S} is the average number of signal counts per first-surface cell and σ_n is the noise (sky-background plus instrument) fluctuation in an adjacent cell not containing the signal of interest, is a useful quantity with which to gauge the relative performances of bare and intensified arrays for short exposure times.

The subsequent analysis, based on the quantity \bar{S}/σ_n , indicated that for exposure times of the order of 0.01 s, the intensified array outperforms the bare array in detection sensitivity for all reasonable (and expected) values of the important parameters - sky brightness, aperture, CCD quantum efficiency, CCD noise, and image-cell size. Should solid-state and electronic technology advance to the point that CCD's become available with image cell counts of the order of 15 rms electrons and with broadband, solar, quantum efficiencies in excess of 50 percent, then the relative-performance conclusions stated above would have to be revised.

In the presentation of the intensified case, ideal conditions were assumed. The current gain was assumed to be noise-free. This is reasonable because of the modest gain requirement. The effect of the increased average background as a result of the pre-array current gain has not been discussed. The distortions and non-uniformities, introduced by the imaging section have been neglected. Their importance remains to be

evaluated in the Laboratory. In a given application in which detection sensitivity is not the major requirement, the stated degrading elements, even though minimized by careful design and fabrication, may well force the decision to use the bare array.

ACKNOWLEDGMENTS

The author wishes to acknowledge discussions with Dr. S. B. Bowling and Dr. V. W. S. Chan of Lincoln Laboratory. In addition, the skillful typing of the manuscript by M. A. Grey is appreciated.

REFERENCES

1. R. Weber, "The Passive, Ground-Based, Electro-Optical Detection of Synchronous Satellites," Technical Note 1978-27, Lincoln Laboratory, M.I.T. (19 June 1978), DDC AD-A059275.
2. R. Weber, "Field-Testing and Evaluation of the TRW Streak MTI System," Project Report ETS-13, Lincoln Laboratory, M.I.T. (9 June 1977), DDC AD-B020022-L.
3. R. Weber, "Visual Magnitude Flux Rate Density Standards for Sunlight Incident on Photoemissive Surfaces," Technical Note 1974-20, Lincoln Laboratory, M.I.T. (6 May 1974), DDC AD-779822/6.

APPENDIX A

With the decision threshold to be set at $k \sigma_n$ above the average background level, expressions for P_{FA} and P_D are as follows:

$$P_{FA} = 1/2 \left[1 - \operatorname{erf} \left(\frac{k}{\sqrt{2}} \right) \right], \text{ and} \quad (A1)$$

$$P_D = 1/2 \left[1 + \operatorname{erf} \left(\frac{\bar{S} - k \sigma_n}{\sqrt{2} \sigma} \right) \right]. \quad (A2)$$

In the expressions developed in the text, k was set equal to j (which essentially determines the value of \bar{S} required for a specified P_D). In the general case for $k \neq j$, \bar{S} is given by:

$$\bar{S} = 1/2 \left[(2k \sigma_n + j^2) + j \sqrt{4 \sigma_n (k + \sigma_n) + j^2} \right]. \quad (A3)$$

Equations A1 - A3 may be applied as follows: Use erf Tables to solve (A1) for k for an acceptable P_{FA} . Insert this k into (A2) and use erf Tables to evaluate the argument of the error function for a desirable P_D . The result at this point will be of the form $\bar{S} - k \sigma_n = \sqrt{2} (\text{Nbr.}) \sigma$. Set $\sqrt{2} (\text{Nbr.}) = j$, where (Nbr.) is the quantity last evaluated. With k and j known, (A3) may be used to calculate the required value of \bar{S} to meet the wanted level of detection performance for various values of σ_n .

As an example, the method just described has been used to evaluate $\bar{S}_m (\sigma_n = 1)$ for an assumed acceptable P_{FA} of 10^{-3} and for a few reasonable values of acceptable P_D 's. The following short table indicates the results.

P_D	\bar{S}_m ($\sigma_n = 1$)
0.999	15.9
.950	8.1
.900	6.7
.750	4.7

A final case, the case for k set at the average reference level (i.e., $k = 0$) is perhaps of interest. Now, the expression (given in the text):

$$\bar{S}_m = k \sigma_n + j \sigma \quad (A4)$$

becomes simply $\bar{S}_m = j \sigma$. Solving for j and making appropriate substitutions, one obtains the familiar

$$j = \frac{\bar{S}_m}{\sigma} = \frac{\bar{S}_m}{\sqrt{\bar{S}_m + (B + N^2)}} \quad (A5)$$

In Eq. (A5), j is a signal to noise-in-signal ratio. At times, the condition that $j \geq 6$ is imposed for detection. The claim is made that this is an unduly restrictive requirement for a real, two-dimensional, scanned system.

Consider a noise-free system in which $(B + N^2) = \sigma_n^2 = 0$. Equation (A5) states that \bar{S}_m for $j = 6$ is 36 counts. True, P_D is essentially unity for $j = 6$ but since for $j = 3$, $P_D \approx 0.999$, the condition is unrealistic. Of course, the analytical P_{FA} for $k = 0$ is exactly one-half for both cases.

For the minimum noise case ($\sigma_n = 1$) considered in the text, \bar{S}_m for $j = 6$ and $k = 0$ corresponds to approximately 37 counts. This, again, is an unreasonably high value for the minimum number of detectable average signal counts for systems of the type discussed. In conclusion, for a system which can tolerate a limited number of false alarms and for which a certain probability of detection per data set is required, appropriate non-zero values of j and k must be used to determine the detection capability of the detector array. Then, signals whose average values are much less than 37 counts are detectable with the wanted and allowed P_D 's and P_{FA} 's; and, the quantity \bar{S}_m/σ_n becomes of first importance.

UNCLASSIFIED

SECURITY CLASSIFICATION OF THIS PAGE (When Data Entered)

19 REPORT DOCUMENTATION PAGE		READ INSTRUCTIONS BEFORE COMPLETING FORM
1. REPORT NUMBER (18) ESD-TR-78-281	2. GOVT ACCESSION NO.	3. RECIPIENT'S CATALOG NUMBER
4. TITLE (and Subtitle) (6) Limiting Point-Source Detection Capabilities of Two-Dimensional, Scanned, Optical Detector Arrays in Constant False-Alarm Systems		5. TYPE OF REPORT & PERIOD COVERED (9) Technical Note
7. AUTHOR(s) (10) Robert Weber		6. PERFORMING ORG. REPORT NUMBER Technical Note 1978-10
9. PERFORMING ORGANIZATION NAME AND ADDRESS Lincoln Laboratory, M.I.T. P.O. Box 73 Lexington, MA 02173		8. CONTRACT OR GRANT NUMBER(s) (15) F19628-78-C-0002
11. CONTROLLING OFFICE NAME AND ADDRESS Air Force Systems Command, USAF Andrews AFB Washington, DC 20331		10. PROGRAM ELEMENT, PROJECT, TASK AREA & WORK UNIT NUMBERS Program Element No. 63428F Project No. 2128
14. MONITORING AGENCY NAME & ADDRESS (if different from Controlling Office) Electronic Systems Division Hanscom AFB Bedford, MA 01731		12. REPORT DATE (11) 3 November 1978
16. DISTRIBUTION STATEMENT (of this Report) Approved for public release; distribution unlimited. (12) 29 P1		13. NUMBER OF PAGES 30
17. DISTRIBUTION STATEMENT (of the abstract entered in Block 20, if different from Report) (14) TN-2978-1A		15. SECURITY CLASS. (of this report) Unclassified
18. SUPPLEMENTARY NOTES None		15a. DECLASSIFICATION DOWNGRADING SCHEDULE
19. KEY WORDS (Continue on reverse side if necessary and identify by block number)		
GEODSS optical point-source detection two-dimensional scanned array single false-alarm threshold signal-to-noise ratio constant false-alarm systems		
20. ABSTRACT (Continue on reverse side if necessary and identify by block number)		
An optical point-source detection system in which a constant number of false alarms is allowed per data set (exposure time) based on the post-detection processing, is considered. The detector is a two-dimensional scanned array. With a single threshold determined solely by the allowed false alarms, that minimum average signal necessary to satisfy a given requirement on the probability of detection for various background (sky, in this instance) and electronic noise levels is determined. This development leads to a critical signal-noise expression at the first photon to charge-carrier conversion surface which is not an explicit function of the standard deviation of the signal. This expression is used to compare the detection performances of noise-free and of noisy detector arrays using the parameters of typical, ground-based, satellite surveillance systems.		

UNCLASSIFIED

SECURITY CLASSIFICATION OF THIS PAGE (When Data Entered)

207 650

elf